Chemical Modification of Palm Fibres Surface with Zirconium Oxychloride

Giulia Araújo Martins,[a] Paulo Henrique Fernandes Pereira,[b] and Daniella Regina Mulinari [a,c]*

Chemical modification of natural fibres has been carried out using different methods for such purposes as reinforcement in polymer matrices and heavy metals adsorption. In this work, palm fibres were modified by zirconium oxychloride *in situ*. The palm fibres that had been chemically modified were compared to those in nature using fibres that passed through 20 and 40 mesh screens to evaluate the influence of particle size on modification. Palm fibres were modified with $ZrO_2.nH_2O$ nanoparticles through the use of zirconium oxychloride in an acidic medium in the presence of palm fibres using ammonium solution (1:3) as the precipitating agent. Scanning electron microscopy (SEM), X-ray diffraction (XRD), infrared spectrophotometry (FTIR), and atomic emission spectrometry with inductively coupled plasma (ICP-AES) were used to characterize the hybrid materials. Results indicated that the particle size of the palm fibres influenced in the modification, because the fibres with smaller particle size had a greater deposition of inorganic material. The ICP technique revealed an increase of 21% nanoparticles $ZrO_2.nH_2O$ deposited on fibres (40 mesh) when compared to fibres (20 mesh). The diameter of nanoparticles $ZrO_2.nH_2O$ deposited on fibres was about 50 to 220 nm, as observed by SEM.

Keywords: Palm fibres; Hydrous zirconium oxide; Nanocomposites

Contact information: a: Department of Engineering, UniFOA, Volta Redonda, Rio de Janeiro, Brazil; b: Department of Materials and Technology, UNESP/FEG, Guaratinguetá/SP, Brazil; c: Department of Mechanic, UERJ/FAT, Resende, Rio de Janeiro, Brazil;
** Corresponding author: daniella.mulinari@foa.org.br*

INTRODUCTION

Recently, much attention has been directed to the development of nanocomposites based on organic-inorganic hybrid materials, such as SiO_2 (Pinto *et al.* 2008), $CaCO_3$ (Vilela *et al.* 2010), $NbOPO_4 \cdot nH_2O$ (Pereira *et al.* 2010,), Nb_2O_5 (Maschio *et al.* 2012), MgO (Maliyekkal *et al.* 2010), silica (Xie *et al.* 2009), TiO_2 (Daoud *et al.* 2005), Al_2O_3 (Alfaya and Gushikem 1999), ZrO_2 (Mulinari and Da Silva 2008), Cel/Sb_2O_3 (Toledo *et al.* 2000), and other applications such as membranes (Biron *et al.* 2012), because these materials normally have improved mechanical, optical, and thermal properties due to the combination of inorganic and organic components.

Organic-inorganic hybrid materials are of more than just academic interest, since their inherent properties frequently lead to the development of innovative industrial applications (Gupta and Sharma 2003; Gupta *et al.* 2006, 2007, 2011, 2012; Gupta and Rastogi 2009). Saleh and Gupta (2012) synthesized manganese dioxide-coated multiwall carbon nanotube (MnO_2/CNT) nanocomposite.

The as-produced nanocomposite was characterized by different characteristic tools, such as X-ray diffraction, SEM, and FTIR. The MnO_2/CNT nanocomposite was utilized as a fixed bed in a column system for removal of lead(II) from water. The experimental conditions were investigated and optimized. The pH range between 3 and 7 was studied; the optimum removal was found when the pH was equal to 6 and 7. The thickness of MnO_2/CNT nanocomposite compact layer was also changed to find the optimum parameter for higher removal. It was observed that the slower the flow rates of the feed solution, the higher was the removal efficiency, and the effect was attributed to a larger contact time.

In this context, hybrid organic-inorganic materials have attracted major interest, since the use of methodologies for nanoparticles, composites, membranes, and nanocomposites, yielded a more economical alternative with greater control for developing new materials to technology applications. Such fields as optics, electronics, ionic, mechanics, energy, environment, biology, medicine, smart coatings, fuel and solar cells, catalysts, sensors, fire retardant, and production of composites or membranes are some examples of areas where these types of materials have been successfully applied (Pereira *et al.* 2011).

Among natural fibres that have been used for the application of these nanocomposites, palm fibres are particularly interesting (Marques *et al.* 2006). Palm trees are considered among the oldest plants on the globe, with records dating back 120 million years. They are a characteristic component of tropical forests and have important features that ensure the sustainable development of agricultural and horticultural systems. The greatest diversity of these plants is in the tropics and subtropics (Belini *et al.* 2011). *Archontophoenix alexandrae*, commonly known as king palm, is a species of the family Aracaceae originally from Queensland, Australia: a tropical region with an altitude below 1100 m. The climate required to cultivate this species is hot and humid. It can, however, adapt to various soil types, from very sandy soils to soils with high clay content, and can tolerate low pH (Ribeiro 1996). The plants of this species form a very dense root system, which makes it very important to prevent erosion of riverbanks.

The heart of palm, also known as palmito, can be extracted from various species of palms. *A. alexandrae* produces heart of palm of the noble type, with higher quality and superior flavor compared to other species of palm. The harvesting of palm heart is done after a period of 4 years (Simas *et al.* 2010). However, a large amount of residue is generated from this cultivation (Simas *et al.* 2010). For each palm, approximately 400 g of commercial palm heart are harvested. The residue constitutes 80 to 90% of the total palm weight, with some variation depending on species (Ribeiro 1996). The residues from king palm are mainly the leaves and leaf sheathes. Some quantity of this highly cellulosic material is currently used as boiler fuel in the preparation of fertilizers or as mulching material, but the majority is left on the mill premises. When left in fields, these waste materials create environmental problems (Shinoja *et al.* 2011). Several studies are seeking to add value to this raw material produced from the extraction of palm heart by using it in other ways.

In this work, $ZrO_2.nH_2O$ particles on palm fibres were investigated using X-ray diffraction (XRD), scanning electron microscopy (SEM), infrared spectrophotometry (FTIR), and atomic emission spectrometry with inductively coupled plasma (ICP-AES) to determine the physical structure, morphological, and chemical properties, and the zirconium content deposited on the fibre surface.

EXPERIMENTAL

Materials and Preparation

Palm fibres were collected from a farm in Volta Redonda (Rio de Janeiro, Brazil). The fibres were dried at 80 °C for 24 h. They were then ground in a mill and sieved to obtain samples that passed through 20 and 40 mesh screens to evaluate the influence of particle size in modification.

For chemical modification of the palm fibres with $ZrO_2.nH_2O$ particles, 2 g of zirconium oxychloride were dissolved in 100 mL of an aqueous hydrochloric acid solution (0.5 mol L^{-1}), in which 5 g of palm fibres were immersed. The material was precipitated with an ammonium solution (1:3) at pH 10.0. The mixture was stirred, filtered, exhaustively washed with distilled water for the complete removal of chloride ions (negative silver nitrate test), and dried at 50 °C for 24 h. The resulting material was designated palm fibre/$ZrO_2.nH_2O$ (Mulinari and Da Silva 2008).

Characterization of Raw Materials and Composites

The physical structure of the palm fibres in nature and modified with $ZrO_2.nH_2O$ particles was evaluated by X-ray diffraction (XRD), Fourier transform infrared (FTIR), scanning electron microscopy (SEM), and atomic emission spectrometry with inductively coupled plasma (ICP-AES).

The crystallinity index was evaluated by X-ray patterns obtained with a Shimadzu diffractometer (model XRD6000) under the following conditions: CuKα radiation with graphite mono-chromator, 40 kV, and 40 mA. Patterns were obtained in the 10 to 70° 2θ angular interval, scanning 0.05 (2θ/5s) for values of 2θ between 10° and 70°. The crystallinity index (CI) was calculated using equation (1), where I_{002} is the maximum intensity of the I_{002} lattice reflection and I_{101} is the maximum intensity of X-ray scattering broad band, due to amorphous region of the sample. This method was developed by Segal *et al.* (1959), and it has been widely used for the study of natural fibres.

$$CI\ (\%) = [I_{002} - I_{101}) / I_{002}] \times 100 \quad (1)$$

Chemical structures of the palm fibres were evaluated by FTIR. The spectrum was obtained on an FTIR spectrophotometer (Perkin Elmer). The samples were prepared by mixing the material and KBr in a proportion of 1:200 (w/w). For each sample, 16 scans were accumulated with a 4 cm^{-1} resolution.

The palm fibre morphology was evaluated with a JEOL JSM5310 scanning electron microscope with a tungsten filament operating at 10 kV, employing the low vacuum technique and secondary electron detector. Samples were dispersed on a brass support and fixed with double-sided 3M tape.

The length and diameter of $ZrO_2.nH_2O$ nanoparticles on palm fibres, uncoated or coated, were measured by quantitative microscopy using the image processing software Image J.

The zirconium content on the palm fibres' surface was quantified by atomic emission spectrometry with inductively coupled plasma (ICP-AES) using a Spectro spectrometer (model Genesis).

RESULTS AND DISCUSSION

Palm fibres are hydrophilic substrates, and therefore their modification with $ZrO_2.nH_2O$ promotes the nucleation and growth of $ZrO_2.nH_2O$ particles. The first step of the reaction was carried out under anhydrous conditions because it is supposed that a donor-acceptor bond is formed between $ZrOCl_2.8H_2O$ and the oxygen of the C_1-O-C_5 and C_1-O-C_4 bonds. The attack to the former oxide bond leads to a ring opening and provides a molecule rupture process to form microfibers, according to the reaction shown in Fig. 1. Ammonium solution is required to promote the chemical link of metallic oxide with fibre surfaces (Mulinari *et al.* 2010).

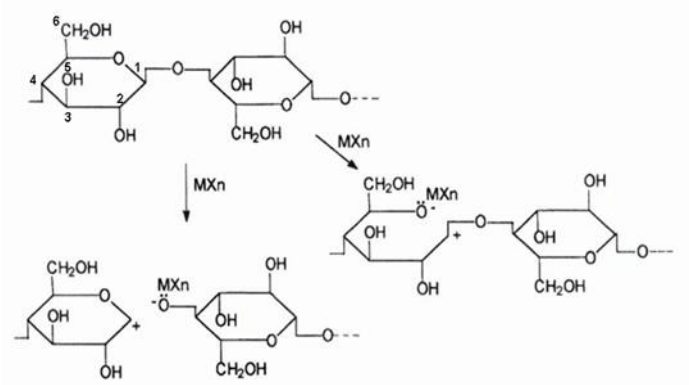

Fig. 1. Reaction of the Lewis acid with cellulose and formation of the donor-acceptor bond (Mulinari *et al.* 2009)

The physical structure of the palm fibres coated with $ZrO_2.nH_2O$ particles was investigated by X-ray diffraction. Analyzing the diffractograms, it was noted that palm fibres presented characteristics of a semicrystalline material, with intense peaks (Fig. 2). On the other hand, a gradual reduction in the peak intensity in the palm fibres coated with $ZrO_2.nH_2O$ particles was observed, and this was attributed to the amorphous character of the $ZrO_2.nH_2O$ (Mulinari *et al.* 2009).

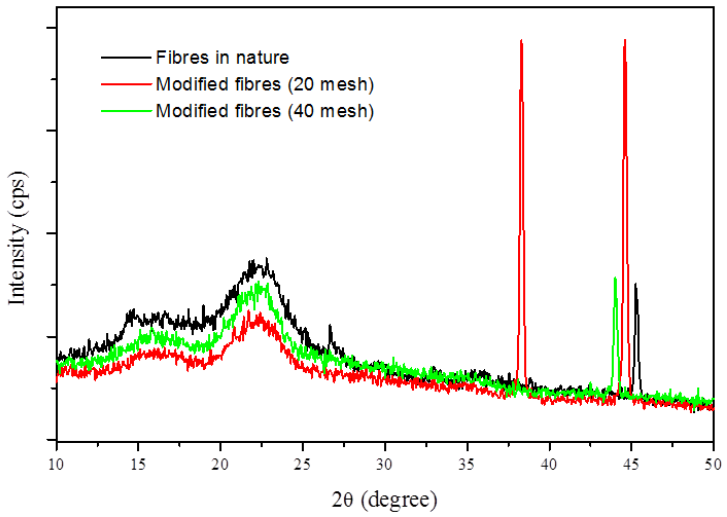

Fig. 2. X-ray diffraction patterns for palm fibres

The spectrum corresponding to the palm fibres in nature showed diffraction peaks at the 2θ angles 14.5° and 22.4°, representing the cellulose crystallographic planes I_{101} and I_{002}. For modified palm fibres, the same peaks were observed at 15.1° and 22.4°. The presence of the peaks at 15° and 22° are evidence of the fibre modification. The position of these peaks indicates an increase of the interplanar distance in relation to the modified fibre. The X-ray diffraction peaks observed can be attributed to crystalline scattering and the diffuse background associated with disordered regions. This behavior occurs because of the generation of disorder when fibres are modified.

The crystallinity index (CI) calculated according to equation (1), can be observed in Table 1. The modified fibres (20 mesh) presented a increase of 5% in the crystallinity index, however the modified fibres (40 mesh) exhibited 39.5% higher crystallinity than fibres in nature. This fact occurred due to the particle size of fibres.

Table 1. Crystallinity Index of Fibres

Material	$I_{(002)}$	$I_{(101)}$	I_c (%)
Fibres in nature	880	613	30.3
Modified fibres (20 mesh)	1012	690	31.8
Modified fibres (40 mesh)	1320	755	42.3

Another technique used for analysis was FT-IR, which reveal the main and typical groups present in the fibres. Figure 3 illustrates the FT-IR spectrum obtained for the palm fibres used in this work. The signals at ~2900 cm^{-1} and ~1700 cm^{-1} are characteristic of the stretching of symmetrical CH groups and the stretching of symmetrical CH groups and the stretching of unconjugated C=O groups present in polysaccharides and xylans. The absorption at 3420 cm^{-1} is due to stretching of C-H groups. In these spectra it was observed around 3400 cm^{-1} the band in the region on the axial O-H stretch. A characteristic band of C-O bonds and C-O-C typical of ethers was observed in the 1150-1000 cm^{-1} region. The band around 1600 cm^{-1} is probably due to the presence of aromatic rings characteristic of lignin. The absorbance ratio of C-O in aromatic ring regions (A1100/A1600) was 1.13, different from that of sugarcane (0.83), showing, in principle, less content of lignin in respect to carbohydrates.

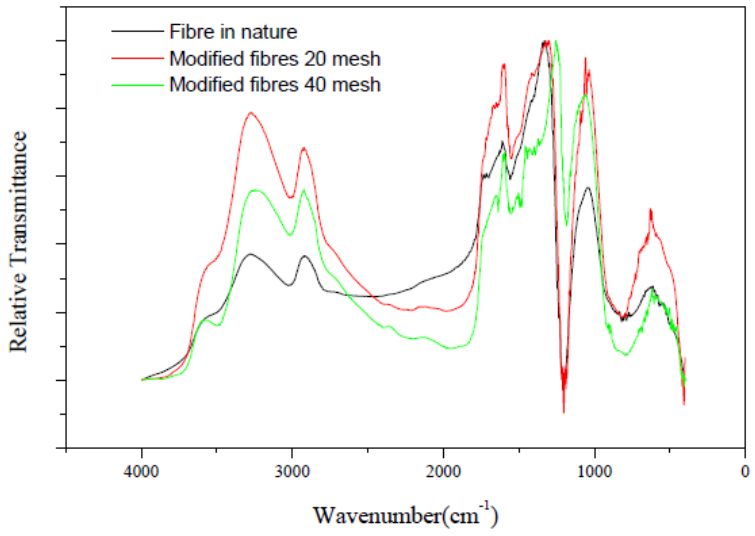

Fig. 3. FTIR spectra of palm fibres

These absorptions are similar to those of sugarcane bagasse fibres (Toledo *et al.* 2000). Table 2 summarizes higher bands observed in the FT-IR spectra of sugarcane bagasse fibres and their assignments to chemical group vibrations and molecules.

Table 2. Infrared Main Transitions for Lignocellulosics Materials

Wavenumber (cm^{-1})	Vibration	Source
3300	O-H linked shearing	Polysaccharides
2885	C-H symmetrical stretching	Polysaccharides
1732	C=O unconjugated stretching	Xylans
1650-1630	OH (water)	Water
1335	C-O aromatic ring	Cellulose
1162	C-O-C asymmetrical stretching	Cellulose
670	C-OH out-of-plane bending	Cellulose

SEM is an excellent technique for examining the surface morphology of palm fibres. The longitudinal and cross-sectional surfaces of palm fibres are presented in Fig. 4, where the presence of lignocellulosic material, hydrophobic non-cellulose compounds (such as waxes), and surface impurities can be observed on the external surface of the cell wall.

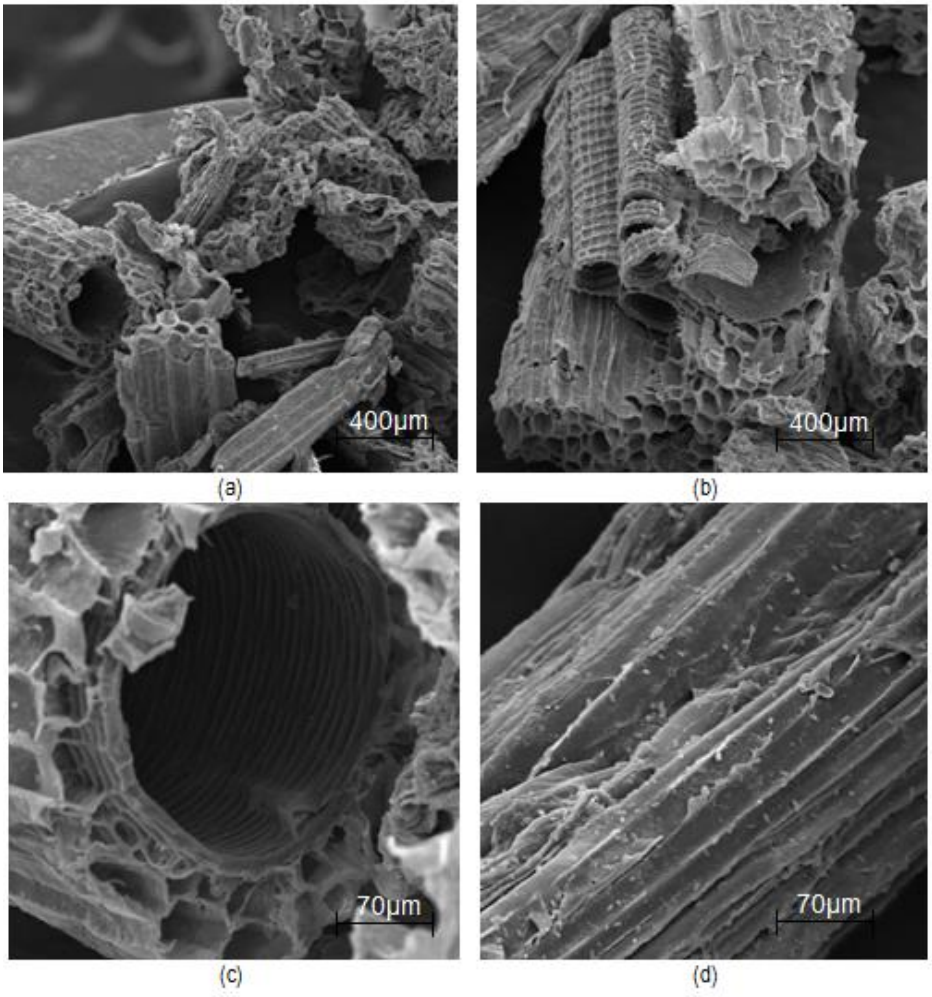

Fig. 4. SEM micrographs of palm fibres *in nature*

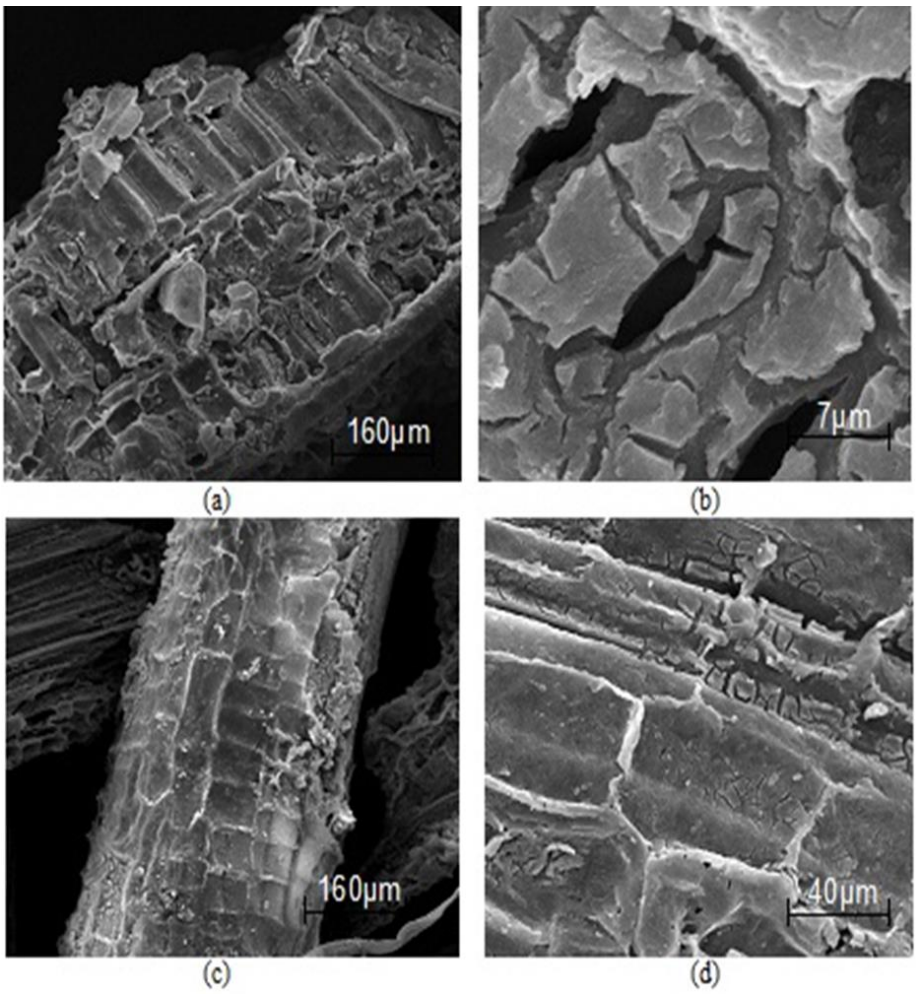

Fig. 5. SEM micrographs of palm fibres modified: 20 mesh (a; b at different magnifications); 40 mesh (c; d at different magnifications)

These compounds constitute a protective and smooth layer on the surface of the fibres. It is also possible to observe a superficial layer of parenchyma cells. Also in Fig. 4 one can observe a smooth surface, but the fibers were porous and cylindrical-shaped.

However, the fibres surface was observed to be covered with oxide, but this did not occur homogeneously (Fig. 5). Figure 5 shows fibres modified with zirconium oxide with different particle size. It was also observed that the particle size of the fibres influenced modification, because the fibres with smaller size had a greater deposition of inorganic material. This fact can be explained by the contact area of the fibres. According to Bittencourt *et al.* (2009), when reducing the particle size, both the surface area and the contact areas between adjacent fibers are increased, decreasing the material size. According to Porte *et al.* (2011), small particles case agglomeration.

A further increase of the fibres allowed the visualization of a greater roughness after modification of the fibre, due to the solubilization of the compounds, facilitating the disintegration of the fibre bundle and increasing the effective surface area. Nanometric particles could be seen on the surface of the fibres. The length of fibres varied from 100 to 500 µm, and the diameter varied from 10 to 30 µm. In the formation of nanoparticles,

$ZrO_2.nH_2O$ nanoparticles in the size range of about 50 to 220 nm in diameter were deposited heterogeneously on fibres.

The ICP technique used in this work was important for determining the content of zirconium deposited on surface of the palm fibres and also to available the influence of particle size in this study. Table 3 shows the zirconium content incorporated in the king palm fibres as a function of particle size.

Table 3. Zirconium Content of Palm Fibre Nanocomposite

Sample	*% ZrO2*
Modified fibres 40 mesh	10.38
Modified fibres 20 mesh	8.5

Results shown in Table 3 confirm the influence of particle size on the deposition of oxide. Fibres prepared with sifted in a 20 mesh sieve, showed a smaller content of zirconium on surface fibres, confirming the study of Bittencourt *et al.* (2009) and Porte e*t al.* (2011).

CONCLUSIONS

1. Synthesis of $ZrO_2.nH_2O$ nanoparticles on palm fibres was carried out successfully. The fibre/$ZrO_2.nH_2O$ nanocomposite was obtained with a high degree of dispersion of hydrous zirconium oxide on the palm fibres' surface.
2. Results showed that the particle size of the fibres influenced modification, such as morphology, crystallinity index, chemical composition, and the amount of zirconium deposited on fibres. Scanning electron microscopy (SEM), X-ray diffraction (XRD), infrared spectrophotometry (FTIR), and atomic emission spectrometry with inductively coupled plasma (ICP-AES) techniques confirmed these results.
3. The $ZrO_2.nH_2O$ nanoparticles on palm fibres can be used reinforcement in matrix polymeric and membranes for nanofiltration.

ACKNOWLEDGMENTS

The authors are grateful for the research support by CAPES.

REFERENCES CITED

Alfaya, R. V. S., and Gushikem, Y. (1999). "Aluminum oxide coated cellulose fibers modified with n-propylpyridinium chloride silsesquioxane polymer: Preparation, characterization and adsorption of some metal halides from ethanol solution," *J. Colloid Interface Sci.* 213(2), 438-444.

Belini, C. M., Bonafim, I. F., and Júnior, R. F. G. (2011). "Crescimento de palmeira real australiana em substratos formulados a partir de composto de poda de árvore," *Revista Biologia Fafibe* 1, 1-10.

Bittencourt, B. A., Ellwanger, M. V., Nascimento, W. A., Belchior, L. F., Araújo, E. M., and Melo, T. J. A (2009). "Moldagem por compressão a frio do polietileno de ultra alto peso molecular," *Polímeros: Ciência e Tecnologia*, 19, 224-230.

Daoud, W. A., Xin, J. H., and Zhang, Y. (2005). "Surface functionalization of cellulose fibers with titanium dioxide nanoparticles and their combined bactericidal activities," *Surf. Sci.* 599(1), 69-75.

Gupta, V. K., and Sharma S. (2003). "Removal of zinc from aqueous solutions using bagasse fly ash—a low cost adsorbent," *Ind. Eng. Chem. Res*. 42(25), 6619-6624.

Gupta, V. K., Mittal, A., Kump, L., and Mittal, J. (2006). "Adsorption of a hazardous dye, erythrosine, over hen feathers," *J. Colloid Interface Sci.* 304(1), 52-57.

Gupta, V. K., Jain, R., Mittal, A., Mathur, M., and Sikarwar, S. (2007). "Photochemical degradation of the hazardous dye safranin-T using TiO_2 catalyst," *J Colloid Interface Sci.* 309(2), 464-469.

Gupta, V. K., Gupta, B., Rastogi, A., Agarwal, S., and Nayak, A. (2011). "A comparative investigation on adsorption performances of mesoporous activated carbon prepared from waste rubber tire and activated carbon for a hazardous azo dye—Acid Blue 113," *J. Hazardous Mater*. 186(1), 891-901.

Gupta, V. K., and Rastogi, A. (2009). "Biosorption of hexavalent chromium by raw and acid-treated green alga *Oedogonium hatei* from aqueous solutions," *J. Hazardous Mater.* 163(1), 396-402.

Gupta, V. K., Ali, I., Saleh, T. A., Nayak, A., and Agarwal, S. (2012). "Chemical treatment technologies for waste-water recycling—an overview," *RSC Adv.* 2, 6380-6388.

Maliyekkal, S. M., Lisha, K. P., and Pradeep, T. (2010). "A novel cellulose–manganese oxide hybrid material by in situ soft chemical synthesis and its application for the removal of Pb(II) from water," *J. Hazardous Mater.* 181(3), 986-995.

Marques, A. A. P., Tito, T., and Pascoal Neto, C. (2006). "Titanium dioxide/cellulose nanocomposite prepared by a controlled hydrolysis method," *Compos. Sci. Technol.* 66(7), 1038-1044.

Maschio, L. J., Pereira, P. H. F., and Da Silva, M. L. C. P. (2012). "Preparation and characterization of cellulose/hydrous niobium oxide hybrid," *Carbohydr.* 89(1), 992-996.

Mulinari, D. R., and Da Silva, M. L. C. P. (2008). "Adsorption of sulphate ions by modification of sugarcane bagasse cellulose," *Carbohydr. Polym.* 74(3), 617-620.

Mulinari, D. R., Voorwald, H. J. C., Cioffi, M. O. H., Da Silva, M. L. C. P., Cruz, T. G., and Saron, C. (2009). "Sugarcane bagasse cellulose/HDPE composites obtained by extrusion," *Compos. Sci. Technol.* 69 (2), 214-219.

Mulinari, D. R., Voorwald, H. J. C., Cioffi, M. O. H., Rocha, G. J. M., and Da Silva, M. L. C. P. (2010). "Surface modification of sugarcane bagasse cellulose and its effect on mechanical and water absorption properties of sugarcane bagasse cellulose/ HDPE composites," *BioResources* 5(2), 661-671.

Pereira, P. H. F., Cioffi, M. O. H., Voorwald, H. J. C., and Da Silva, M. L. C. P. (2010). "Preparation and characterization of celulose/ hydrous niobium phosphate hybrid," *BioResources* 5(2), 1010-1021.

Pereira, P. H. F., Cioffi, M. O. H., Voorwld, H. J. C., and Da Silva, M. L. C. P. (2011). "Novel cellulose/$NbOPO_4.nH_2O$ material from sugarcane bagasse," *BioResources* 6(1), 867-878.

Pereira, P. H. F., Cioffi, M. O. H., Voorwald, H. J. C., Mulinari, D. R., Luz, S. M., and Da Silva, M. L. C. P. (2011). "Sugarcane bagasse pulping and bleaching: Thermal and chemical characterization," *BioResources* 6(3), 2471-2482.

Pinto, R. J. B., Marques, P. A. A. P., Barros-Timmons, A. M., Trindade, T., and Pascoal Neto, C. (2008). "Novel SiO_2/cellulose nanocomposites obtained by in situ synthesis andvia polyelectrolytes assembly," *Composites Science and Technology* 68(1), 1088-1093.

Porte, L. H. M., Leão, M. H. M. R., and Porte, A. (2011). "Avaliação da porosidade de microcápsulas contendo proteína bioativa por porosimetria de mercúrio e adsorção de nitrogênio," *Química Nova* 34, 1582-1587.

Ribeiro, J. H. (1996). "SOS palmito," *Revista Globo Rural* 3, 24-26.

Saleh, T. A., and Gupta, V. K. (2012). "Column with CNT/magnesium oxide composite for lead (II) removal from water," *Environ Sci Pollut Res.* 19(4), 1224-1228.

Simas, K. N., Vieira, L. N., Podestá, R., Vieira, M. A., Rockenbach, I. I., Petkowicz, L. O., Medeiros, J. D., Francisco, A., Amante, E. R., and Amboni, R. D. M. C. (2010). "Microstructure, nutrient composition and antioxidant capacity of king palm flour: A new potential source of dietary fibre," *Biores. Technol.* 101(14), 5701-5707.

Shinoja, S., Visvanathanb, R., Panigrahic, S., and Kochubabua, M. (2011). "Oil palm fiber (OPF) and its composites: A review," *Industrial Crops and Products* 33(1), 7-22.

Toledo, E. A., Gushikem, Y., and Castro, S. C. (2000). "Antimony(III) oxide film on a cellulose fiber surface: Preparation and characterization of the composite," *Journal Colloid Interface Science* 225(2), 455-459.

Vilela, C., Freire, C. S. R., Marques, P. A. A. P., Trindade, T., Pascoal Neto, C., and Fardim, P. (2010). "Synthesis and characterization of new $CaCO_3$/cellulose nanocomposites prepared by controlled hydrolysis of dimethylcarbonate," *Carbohydrate Polymers* 79(4), 1150-1156.

Xie, K., Yu, Y., and Shi, Y. (2009). "Synthesis and characterization of cellulose/silica hybrid materials with chemical crosslinking," *Carbohydrate Polymers* 78(4), 799-805.

Article submitted: March 14, 2013; Peer review completed: September 20, 2013; Revised version received and accepted: October 7, 2013; Published: October 22, 2013.